# A Relaxation Solution of Transonic Nozzle Flows Including Rotational Flow Effects

E. F. Brown*
*Virginia Polytechnic Institute and State University, Blacksburg, Va.*
T. J. F. Brecht†
*Union Carbide Technical Center, South Charleston, W. Va.*
and
K. E. Walsh‡
*Hercules, Inc., Cumberland, Md.*

**A computational procedure is described for rotational transonic flows. The effects of rotationality were introduced by a rotation function, and the resulting "potential-like" equation was solved by type-dependent relaxation. The method has been used to predict the flowfield in propulsion-type nozzles using both arbitrarily specified and experimentally measured entrance conditions. In these runs, good agreement with analysis and available experimental results was obtained, and a significant influence due to the rotationality of the flow was observed.**

## Introduction

NONUNIFORMITIES in total pressure and total temperature at the exhaust nozzle entrance produced by nonuniform combustion, heat transfer, flow separation, and mixing of core and fan flows produce significant effects on nozzle performance. Wehofer and Matz[1] tested several typical turbofan exhaust nozzle configurations with nonuniform entrance conditions, and their tests showed that total pressure gradients could cause the discharge coefficient to vary up to 2% and the thrust coefficient to vary up to 3% from the values obtained with uniform entrance flow. Tests conducted with both total pressure and total temperature nonuniformities indicated that total temperature gradients could cause an additional 1% change in discharge coefficient and a 3% change in thrust coefficient. It is clear, therefore, that such entrance flow nonuniformities must be taken into account to predict exhaust nozzle performance accurately.

Several methods for solving transonic flow problems have been developed. Brown and Hamilton[2] present a review of many of these methods. However, only a few of these methods permit rotational flow. Since rotation can be related to nonuniform stagnation properties by Crocco's theorem,[3] ignoring rotational effects is equivalent to ignoring the nonuniform inlet flow effects mentioned in the preceding paragraph.

Ferri and Dash included the effects of nonuniformities in entrance stagnation conditions in their indirect method.[4] Their calculations, which used a coarse grid, show a 1 to 2% variation in thrust caused by flow nonuniformities. Indirect methods, however, have the disadvantage that repeated calculations are necessary to obtain the solution corresponding to the desired nozzle geometry, and in certain cases the convergence of this process is not assured.

Wehofer and Moger[5,6] have developed a time-dependent method for the solution of rotational transonic nozzle flow problems. Their calculations show effects due to nonuniformities in stagnation conditions of approximately 5% in discharge coefficient and approximately 4% in thrust coefficient. However, most time-dependent methods suffer the disadvantage of long computational time. Brown and Hamilton[2] indicate that time-dependent methods can require as much as an order of magnitude more computational time than, for example, relaxation methods.

Emmons[7] used relaxation methods in 1944 to solve transonic flow problems by hand calculation. However, because of stability problems, relaxation methods were unsuccessful in computerized calculations until Murman and Cole[8] in 1970 introduced type-dependent finite differencing, that is, a differencing scheme that takes into account the local type of the governing equations. Since then many other investigators have used relaxation methods; however, applications of the relaxation method have been primarily to external flows such as transonic airfoil problems. Moreover, many relaxation solutions employ the small-disturbance equations of transonic flow rather than the full potential equations. Clearly the small-perturbation assumption is inappropriate for propulsion nozzle problems wherein the Mach number may range from 0.4 at the entrance to 1.4 in the exhaust jet. This paper describes a modification of existing full-potential external-flow relaxation methods for the problem of determining exhaust nozzle performance and a novel extension of relaxation methods to include rotational flow effects.

## Governing Equations

In the absence of viscosity, heat conduction, and body forces, steady compressible fluid flow can be described by Euler's equation,

$$(V\cdot\nabla)V=-(1/\rho)\nabla P \tag{1}$$

and the continuity equation,

$$\nabla\cdot(\rho V)=0 \tag{2}$$

where $V$ is the velocity vector, $P$ the static pressure, and $\rho$ the density. It is well known that, for the axially symmetric, steady, isentropic flow of an ideal gas, these equations can be simplified by the use of the potential function $\phi'(x,r)$, where

Presented as Paper 76-647 at the AIAA/SAE 12th Propulsion Conference, Palo Alto, Calif., July 26-29, 1976; submitted Sept. 13, 1976; revision received June 10, 1977.

Index categories: Airbreathing Propulsion; Nozzle and Channel Flow; Transonic Flow.

*Associate Professor, Mechanical Engineering Department. Member AIAA.

†Engineer, Heat Transfer and Fluid Dynamics Group.

‡Senior Engineer, Alleghany Ballistics Laboratory.

$\phi'$ is defined by

$$\frac{\partial \phi'}{\partial x} \equiv u \qquad \frac{\partial \phi'}{\partial r} \equiv v$$

where $u$ is the $x$ component of velocity, and $v$ is the $r$ component of velocity. The resulting equation of motion is

$$(c^2 - \phi_x'^2)\phi_{xx}' + (c^2 - \phi_r'^2)\phi_{rr}' - 2\phi_x'\phi_r'\phi_{xr}' + (c^2/r)\phi_r' = 0$$

where subscripts indicate partial differentiation, and the sonic speed $c$, is given in terms of the stagnation speed of sound $c_0$ by

$$c^2 = c_0^2 - [(\gamma - 1)/2](\phi_x'^2 + \phi_r'^2)$$

where $\gamma$ is the ratio of specific heats.

These equations, which are valid only for irrotational flow, can be extended to rotational flow (excluding the effects of viscosity, shocks, and thermal conductivity) by introducing the rotation function $F(x,r)$ and defining a velocity function $\phi$ such that

$$\phi_x + F \equiv u \tag{3}$$

$$\phi_r \equiv v \tag{4}$$

where $u$ and $v$ have been nondimensionalized with respect to the local stagnation speed of sound, and $x$ and $r$ have been nondimensionalized with respect to the radius of the outer wall at the throat. The velocity components $u$ and $v$ are represented in terms of the derivatives of the velocity function (analogous to the potential function introduced previously) in order to combine Eqs. (1) and (2) into a single partial differential equation of second order, thereby simplifying the numerical calculations and the treatment of the boundary conditions. Although the authors are unaware of any direct reference to the type of governing equations which introduction of this representation of the velocity components produces, this procedure is roughly similar to the classical decomposition of a vector field into irrotational and solenoidal components.

As is shown in the Appendix, Eqs. (1) and (2) can be reduced to the nondimensional equation

$$[c^2 - (\phi_x + F)^2](\phi_{xx} + F_x) + [c^2 - (\phi_r)^2](\phi_{rr}) - (\phi_x + F)(\phi_r)(2\phi_{xr} + F_r) + (c^2/r)(\phi_r) = 0 \tag{5}$$

where

$$c^2 = 1 - [(\gamma - 1)/2][(\phi_x + F)^2 + (\phi_r)^2]$$

By differentiating Eq. (3) with respect to $r$ and Eq. (4) with respect to $x$, the function $F$ can be related to the local rotation $\omega$ by $F_r = \omega$, where

$$\omega \equiv \frac{\partial u}{\partial r} - \frac{\partial v}{\partial x}$$

As is shown in the Appendix, Crocco's theorem[3] can be used to find a relationship between the rotation function and the radial variation of total pressure $P_0$ which is given by

$$F_r = \frac{1}{u\gamma P_0}\left(1 - \frac{\gamma - 1}{2} M_0^2\right)\frac{\partial P_0}{\partial r} \tag{6}$$

where $M_0$ is the velocity divided by the stagnation speed of sound.

A knowledge of the total pressure at each point in the flowfield is needed in Eq. (6). For steady flow under the assumption of negligible viscosity, body forces, and heat conduction, the total pressure is constant along streamlines. Thus the local value of the total pressure can be determined by simply tracking streamlines and using the fact that the total pressure along each streamline is known from the total pressure distribution supplied at the entrance.

Equations (5) and (6) are independent of the total temperature because nondimensionalization caused terms involving total temperature to cancel. Thus local Mach numbers and flow angles are independent of total temperature gradients. This result is confirmed by Ferri and Dash[4] and Taulbee and Boraas.[9] However, this does not imply that performance coefficients are independent of the total temperature profile. Once a solution of the governing equation is obtained, the total temperature profile must be considered in the determination of the average total temperature used in the definition of the discharge coefficient. Note that Eqs. (5) and (6) are not in conservative form, and thus the value of the discharge coefficient can be expected to vary slightly with axial position.

## Coordinate Transformation

There are three reasons for using the transformation from the physical plane to the computational plane shown in Fig. 1. First, the transformation results in a rectangular computational grid. This avoids the complication of irregular finite-difference molecules at the nozzle wall. Second, a computational plane of equally spaced mesh points provides greater accuracy that can be obtained by using unequal mesh spacing.[10] Third, the coordinate transformation enhances computational stability in the supersonic region. This is because one axis of the computational plane is approximately aligned with the flow direction. Thus the backward finite difference, which is discussed in the next section, also is approximately aligned with the flow. Thus stability is achieved without the use of a rotated difference scheme in the supersonic region such as used by South and Jameson.[11]

The coordinate transformation used was

$$\xi = \xi(x) = x/L$$

$$\psi = \psi(x,r) = (r - R_i)/(R_0 - R_i)$$

The derivatives of the velocity function and the rotation function can be transformed from the physical coordinates to the computational coordinates by application of the chain rule. This gives rise to the following governing differential equation in the transformed coordinates:

$$A\phi_{\xi\xi} + B\phi_{\xi\psi} + C\phi_{\psi\psi} = D \tag{7}$$

where

$$A = [c^2 - (\phi_x + F)^2]\xi_x^2 \tag{8a}$$

$$B = 2[c^2 - (\phi_x + F)^2]\xi_x\psi_x - 2(\phi_x + F)(\phi_r\xi_x\psi_r) \tag{8b}$$

$$C = [c^2 - (\phi_x + F)^2]\psi_x^2 + (c^2 - \phi_r^2)\psi_r^2 - 2(\phi_x + F)\phi_r\psi_x\psi_r \tag{8c}$$

$$D = (\phi_x + F)\phi_r F_r - (c^2/r)\phi_r - [c^2 - (\phi_x + F)^2](F_x + \phi_\psi\psi_{xx}) + 2(\phi_x + F)\phi_r\phi_\psi\psi_{xr} \tag{8d}$$

and where

$$\xi_x = 1/L \qquad \xi_{xx} = 0$$

$$\psi_x = -\frac{1}{R_0 - R_i}\frac{dR_i}{dx} - \frac{r - R_i}{(R_0 - R_i)^2}\left(\frac{dR_0}{dx} - \frac{dR_i}{dx}\right)$$

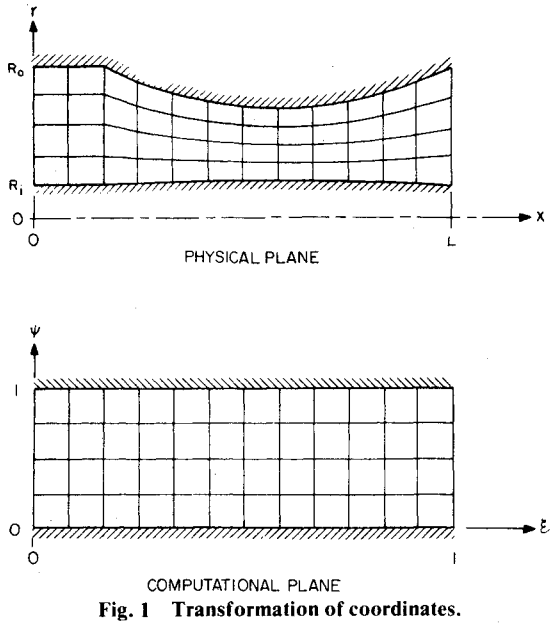


**Fig. 1 Transformation of coordinates.**

$$\psi_{xx} = -\frac{1}{R_0 - R_i}\frac{d^2R_i}{dx^2} + \frac{2}{(R_0 - R_i)^2}\frac{dR_i}{dx}\left(\frac{dR_0}{dx} - \frac{dR_i}{dx}\right)$$

$$-\frac{r - R_i}{(R_0 - R_i)^2}\left(\frac{d^2R_0}{dx^2} - \frac{d^2R_i}{dx^2}\right)$$

$$+2\frac{r - R_i}{(R_0 - R_i)^3}\left(\frac{dR_0}{dx} - \frac{dR_i}{dx}\right)^2$$

$$\psi_r = 1/(R_0 - R_i) \qquad \psi_{rr} = 0$$

$$\psi_{rx} = -\frac{1}{(R_0 - R_i)^2}\left(\frac{dR_0}{dx} - \frac{dR_i}{dx}\right)$$

## Relaxation Procedure

The transformed governing equations were solved numerically using finite-difference expressions to approximate the derivatives. To assure that the domain of dependence of the resulting algebraic equations matched that of the original partial differential equations, both centered and backward finite differences were used. In accordance with standard type-dependent relaxation methods, all derivatives in the subsonic region were evaluated by centered finite-difference (second-order accurate) expressions. Radial derivatives in the supersonic region also were evaluated by centered differences. However, the axial derivatives ($\phi_\xi$ and $\phi_{gg}$) were evaluated by backward finite differences, with the first derivative expressions being second-order accurate and the second derivative expressions being only first-order accurate. (The second-order accuracy of the first derivatives represents a departure from conventional transonic relaxation techniques.) Upon introducing these finite-difference forms, Eq. (7) becomes

$$A\frac{\phi_{i-1,j} - 2\phi_{i,j} + \phi_{i+1,j}}{(\Delta\xi)^2}$$

$$+B\frac{\phi_{i+1,j+1} - \phi_{i-1,j+1} - \phi_{i+1,j-1} + \phi_{i-1,j-1}}{4\Delta\xi\Delta\psi}$$

$$+C\frac{\phi_{i,j-1} - 2\phi_{i,j} + \phi_{i,j+1}}{(\Delta\psi)^2} = D \qquad (9)$$

for subsonic flow. A similar equation is obtained for supersonic flow:

$$A\frac{\phi_{i-2,j} - 2\phi_{i-1,j} + \phi_{i,j}}{(\Delta\xi)^2} + B\frac{\phi_{i-2,j+1} - 4\phi_{i-1,j+1} + 3\phi_{i,j+1}}{4\Delta\xi\Delta\psi}$$

$$-B\frac{\phi_{i-2,j-1} - 4\phi_{i-1,j-1} + 3\phi_{i,j-1}}{4\Delta\xi\Delta\psi} + C\frac{\phi_{i,j-1} - 2\phi_{i,j} + \phi_{i,j+1}}{(\Delta\psi)^2} = D \qquad (10)$$

Values of $A$, $B$, $C$, and $D$ are given as functions of $\phi$ by Eq. (8). Considering just the $i$th column, Eqs. (9) and (10) can be written in matrix form as

$$A_i(\phi)\,\phi_i = f(\phi)$$

where $A_i$ is a tridiagonal coefficient matrix containing the terms $A$, $B$, and $C$; $\phi_i$ is the column vector of unknown $\phi$'s:

$$\phi_i = \begin{bmatrix} \phi_{i,1} \\ \phi_{i,2} \\ \vdots \\ \phi_{i,j\max-1} \\ \phi_{i,j\max} \end{bmatrix}$$

and $f$ is a column vector containing $A$, $B$, and $D$, values of $\phi$ upstream and downstream of the $i$th column, and the image values $\phi_{i,j\max+1}$ and $\phi_{i,0}$. Thus both $A$ and $f$ are functions of $\phi$.

Since the coefficient matrix $A$ is tridiagonal, the solution

$$\phi_i = A_i^{-1} f \qquad (11)$$

can be obtained by the Thomas algorithm. The latest available values of $\phi$ are used to calculate $A$ and $f$. Then Eq. (11) is solved for $\phi_i$. Next, the relationship

$$\lambda\phi_i^{l+1} + (1-\lambda)\phi_i^{l}$$

where $\lambda$ is the column under-relaxation factor and $l$ is the iteration number, is applied to these results, and the underrelaxed values are used to replace the $\phi$ values in the $i$th column. Then the values of $\phi$ at image points of the $i$th column are calculated by the method described in the following section.

This successive relaxation procedure is applied once to each column, starting at the entrance and proceeding to the exit. After the last column has been reached, the relationship

$$\Lambda\phi_i^{l+1} + (1-\Lambda)\phi_i^{l}$$

where $\Lambda$ is the nozzle relaxation factor, is used to update all values of $\phi$.

Two relaxation formulas are required to provide stability and fast convergence. The relaxation factors possess values above which the calculations become unstable. "Safe" values of the relaxation factors were found to vary with nozzle geometry. A value of $\lambda$ of 0.8 produced stable calculations for all geometries tested. For this value of $\lambda$, the value of $\Lambda$ used was 1.0 in the subsonic region and 0.9 in the supersonic region.

After updating all values of $\phi$, $F$ values are re-evaluated. This is done by application of the relationship

$$F_r = \frac{1}{u\gamma P_0}\left(1 - \frac{\gamma - 1}{2}M_0^2\right)\frac{\partial P_0}{\partial r}$$

which is repeated here from Eq. (6). Since $F$ at the centerline or centerbody is known from the boundary conditions, $F$ at any point in the flowfield can be determined by integrating Eq. (6) using, for example, the trapezoidal rule:

$$F_{i,j} = F_{i,j-1} + \left( \frac{(F_r)_{i,j-1} + (F_r)_{i,j}}{2} \right) \frac{\Delta\psi}{\psi_r}$$

The updated values of $\phi$ and $F$ are used to recalculate the total pressure at each computational point. This procedure involves calculating the mass flow between the point at which the total pressure is to be determined and the centerbody or centerline. Then this mass flow is compared with the entrance mass flow to determine which streamline passes through that point. The value of the total pressure at that point then is equal to the total pressure which that streamline possesses at the nozzle entrance (the entrance values of total pressure being supplied as input to the calculations).

Based upon the new values of $\phi$ and $F$, values of $\phi$ at all image points are recalculated using the same procedure as previously described, and the relaxation procedure is repeated until the maximum change in Mach number for 100 iterations is less than some specified value, usually 0.001.

## Boundary Conditions

Proper boundary conditions must be applied to assure the existence of a unique solution of the governing equations. For the problem of transonic nozzle flow, conditions at the wall, entrance, and centerline (or centerbody) are required. Since only solutions with supersonic exit flow are desired, no exit boundary condition is required.

At the nozzle entrance, a constant area section with walls parallel to the axis was added. At the beginning of this constant area section, the velocity function was set equal to a constant. This is equivalent to specifying zero radial velocity. Also, at this location the total pressure (either assumed or obtained from experiment) was specified as a function of radius.

For the application of boundary conditions at the walls, image points were established one mesh space past the walls. The image points are denoted $\phi_{i,0}$ (centerline, or centerbody wall) and $\phi_{i,j\max+1}$ (outer wall). The values of $\phi$ at these image points are specified such that the tangency condition

$$\frac{v}{u} = \frac{\phi_r}{\phi_x + F} = \frac{\mathrm{d}R}{\mathrm{d}x}$$

is met. In terms of the computational coordinates this becomes

$$\left( \frac{\partial\phi}{\partial\psi} \frac{\partial\psi}{\partial r} \right) \Big/ \left( \frac{\partial\psi}{\partial\xi} \frac{\partial\xi}{\partial x} + \frac{\partial\phi}{\partial\psi} \frac{\partial\psi}{\partial x} + F \right) = \frac{\mathrm{d}R}{\mathrm{d}x}$$

Rearrangement yields

$$\frac{\partial\phi}{\partial\psi} = \frac{\mathrm{d}R}{\mathrm{d}x} \left( \frac{\partial\phi}{\partial\xi} \frac{\partial\xi}{\partial x} + F \right) \Big/ \left( \frac{\partial\psi}{\partial r} - \frac{\mathrm{d}R}{\mathrm{d}x} \frac{\partial\psi}{\partial x} \right)$$

Application of centered finite differences permits solving for the values of the velocity function at the image points:

$$\phi_{i,j\max+1} = \phi_{i,j\max-1} + 2\Delta\psi \frac{\partial\phi}{\partial\psi}$$

$$\phi_{i,0} = \phi_{i,2} - 2\Delta\psi \frac{\partial\phi}{\partial\psi}$$

Use of image points to satisfy the boundary conditions permits all points in the flowfield to satisfy the governing equations.

Equation (5) requires special treatment at the centerline because it contains the indeterminate term, $(c^2/r)\phi_r$. Application of l'Hôpital's rule yields

$$\lim_{r\to 0} \frac{c^2}{r} \phi_r = c^2 \phi_{rr}$$

Thus, Eq. (5) reduces to

$$[c^2 - (\phi_x + F)^2](\phi_{xx} + F_x) + 2c^2\phi_{rr} = 0$$

at the centerline.

A boundary condition must be specified for $F$ on some curve not tangent to the radial direction. Mathematical theory provides little guidance in the proper selection of the boundary condition on $F$. Thus two procedures were investigated. In one, the value of $F$ on the centerline/centerbody of the nozzle was set equal to zero. In the other, the value of $F$ on the centerline/centerbody was set equal to the axial component of the local velocity. Although it can be argued that the second boundary condition does not, in fact, represent an independent specification of $F$, it was found to produce superior results from the standpoint of the attainment of mass conservation. Further discussion of this matter appears in the following section.

## Results

The procedure described in the preceding sections was coded in Fortran IV and, when run on an IBM 370/158 computer, requires a region size of approximately 170K. The coding was given the acronym RETIRE (RElaxation of Transonic Flows Including Rotational Effects). In order to reduce computational time, a mesh-halving procedure similar to that devised by South and Jameson[11] was used. Parabolic interpolation was used to determine values of $\phi$, $F$, and $P_0$ at the intermediate points. The mesh-halving procedure can be repeated as often as desired until the array space is exceeded. Typically a solution starts with a $13\times6$ mesh, proceeds to a $25\times11$ mesh, and ends with a $49\times21$ mesh. Additional programming features include subroutines to compute lines of constant Mach number (by means of linear interpolation) and compute the discharge coefficient (based on mass-flow weighted average values of total temperature and total pressure).

The results of three runs will be described. In all cases, the flow is choked. The nozzle geometries shown in Fig. 2 consist of 1) a hyperbolic convergent-divergent nozzle, 2) a conical convergent-divergent nozzle tested by Wehofer and Moger,[6] and 3) a typical turbofan bypass nozzle. Incidentally, no special attempt was made to resolve the discontinuities in wall slope shown in this figure. In fact, the transformation derivatives were computed by finite-difference expressions which, in effect, ignored these discontinuities and replaced the actual wall shape by a series of second-order polynomials.

In order to compare the results of the present program with a well-documented analytical solution, the results for uniform (irrotational) flow in a hyperbolic convergent-divergent nozzle are shown in Fig. 3, along with the calculations of Oswatitsch and Rothstein.[12] The solid lines represent lines of constant Mach number obtained with the present program. Agreement between the two results is good. The figure also shows the computed results for two different mesh sizes, a $25\times11$ mesh and a $49\times21$ mesh. The similarity of results indicates the lack of dependence of the solution on mesh size.

Since the finite-difference form of the governing equations that the program solves are not in conservative form, the solution of the equations does not obey conservation of mass exactly. The calculated mass flow at one axial location might be slightly different from the calculated mass flow at another axial location. However, as the mesh size is reduced, the variation in the calculated mass flow decreases. It is seen in

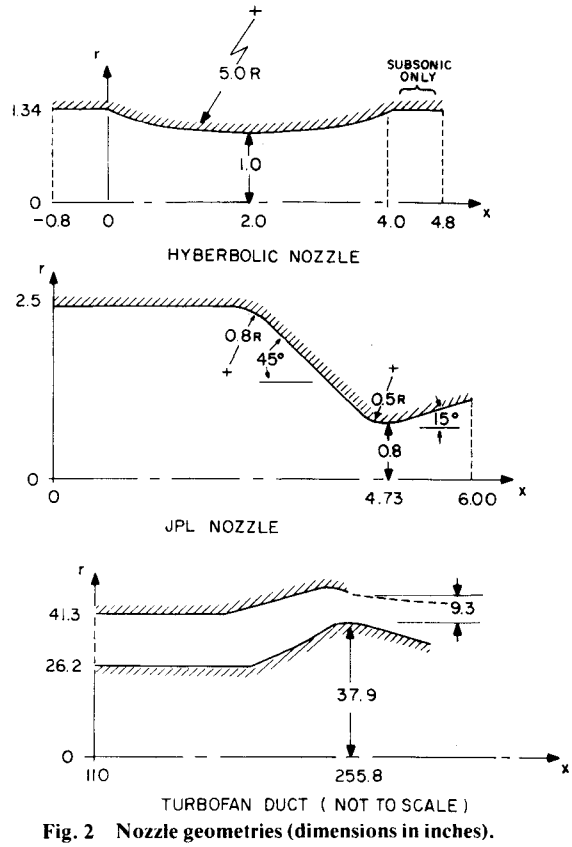


**Fig. 2 Nozzle geometries (dimensions in inches).**

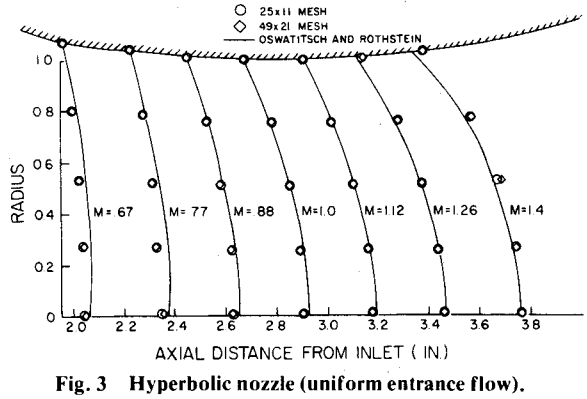


**Fig. 3 Hyperbolic nozzle (uniform entrance flow).**

Fig. 4 that, as the mesh spacing is reduced, the mass flow (actually the discharge coefficient) approaches a constant value. The discharge coefficient is defined by the equation

$$C_D = \frac{\int \rho u 2\pi r dr}{\rho^* V^* \pi (R_{th}^2 - r_{th}^2)}$$

where the asterisk represents sonic values, and $R_{th}$ and $r_{th}$ are wall and centerbody radii at the geometric throat. At the throat ($x=2.8$), the computed value of discharge coefficient does not vary with mesh size. Therefore, the discharge coefficient calculated at the throat can be considered to be a reliable prediction of the discharge coefficient of the nozzle regardless of mesh spacing. Also illustrated in Fig. 4 are the effects on discharge coefficient of two different specifications of $F$ at the centerline. In one case, the centerline values of $F$ are zero at all axial positions. In the other case, the centerline values of $F$ are set equal to the axial velocities. The latter specification resulted in a significantly reduced variation of the discharge coefficient. In accordance with these results, the axial-velocity boundary condition on $F$ was used in all subsequent runs except where otherwise noted.

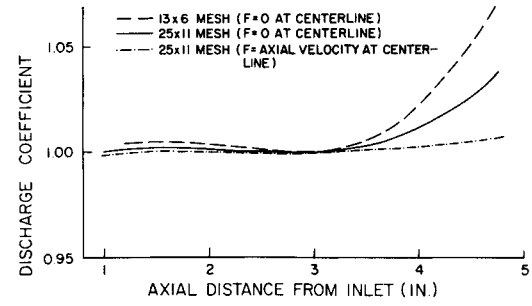


**Fig. 4 Variation of discharge coefficient with axial location (hyperbolic nozzle).**

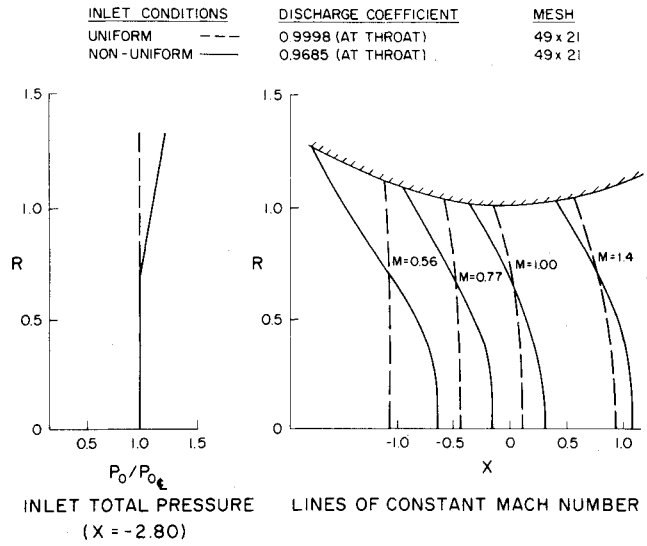


**Fig. 5 Hyperbolic nozzle (nonuniform entrance flow).**

Figure 5 shows the effect of an arbitrary total pressure gradient on isomach lines in the same hyperbolic nozzle. The 25% maximum variation in the total pressure caused a significant shift in the lines of constant Mach number and a 1% decrease in discharge coefficient. In this case, the effects of the total pressure gradient on the discharge coefficient were greater by two orders of magnitude than the effect of two-dimensionality, which caused an almost insignificant 0.02% decrease in the mass flow rate from the one-dimensional value of unity.

Wehofer and Moger[5] have published the results of their time-dependent calculations and their measurements of the flow in a conical convergent-divergent nozzle. Figure 6 shows that the results of the RETIRE program agree well with their analytical and experimental results. The discharge coefficient calculated by Wehofer and Moger included a boundary-layer correction. Since RETIRE does not include a boundary-layer correction, a discharge coefficient slightly higher than either Wehofer and Moger's analytical value or their experimental value is to be expected.

In all fairness, it must be admitted that the results shown in Fig. 6 are not conclusive proof of the ability of the present program to handle nonuniform entrance flows accurately. This is because there is only a 6% variation in total pressure, and therefore the results for nonuniform entrance flow differ only slightly from the uniform entrance flow results. For example, calculations reveal that the discharge coefficient for uniform flow was 0.972 compared to 0.974 for nonuniform inlet flow, and the maximum difference in wall static pressure between the two results was only about 1%. Therefore, it was decided to run a case in which significant entrance flow nonuniformity was present.

The case selected was the flow in a turbofan exhaust nozzle in which the entrance total pressure profile was available from

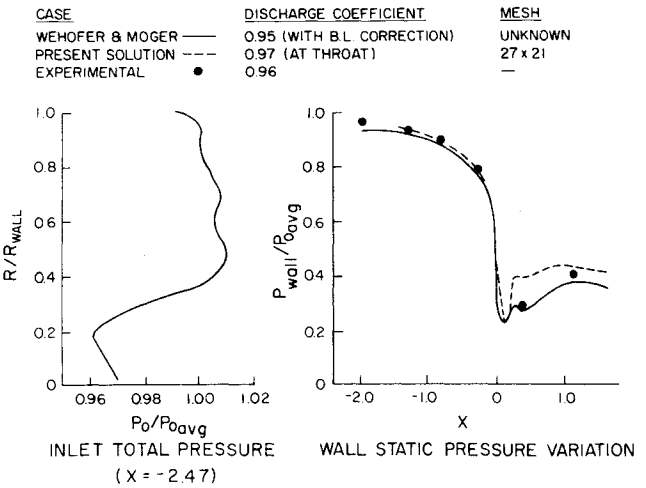


**Fig. 6 Concial convergent-divergent nozzle.**

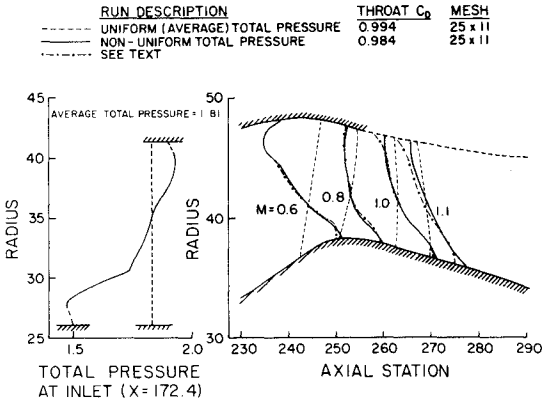


**Fig. 7 Turbofan exhaust nozzle.**

actual in-flight measurements. Two modifications of the original data were required to render them suitable for use in the present program: 1) because the original nozzle had an insufficient divergent section to produce supersonic flow at the exit (as required by the program), a divergent section was added, as shown by the dashed lines in Fig. 7; and 2) since wall values of the total pressure were not supplied, values were extrapolated as indicated by the dashed lines in the left portion of this figure.

Figure 7 shows that the total pressure gradient resulted in a large shift in the lines of constant Mach number and a 1% decrease in the discharge coefficient. This clearly demonstrates that in this actual aircraft-application case the effects of entrance flow nonuniformities cannot be neglected.

As a final demonstration of the effect on the solution of the selection of the boundary condition on $F$, the nonuniform inlet flow case described previously was rerun with the $F=0$ boundary condition. These results also are shown in Fig. 7. Although a slightly different value of the discharge coefficient (0.979) should be expected as a result of the poor mass conservation experienced with the boundary condition, the position of the lines of constant Mach number are virtually unchanged from the previous results.

Finally, a word should be mentioned about the computational speed of the program. Computational times varied from 0.2 sec/point for the hyperbolic nozzle (49×21 mesh, uniform entrance flow) to 1.1 sec/point for the turbofan bypass nozzle (25×11 mesh, nonuniform entrance flow). This represents from 300 to 1200 iterations.

## Conclusions

The results of this research indicate the importance of including the effects of entrance flow nonuniformities in evaluating propulsion nozzle performance and the feasibility and accuracy of extending conventional relaxation methods to account for these effects in a computationally efficient manner.

## Appendix

In preparation for the development of the governing equations, certain preliminary facts and relationships must be established. The first of these is that for flow of a chemically homogeneous substance in the absence of heat conduction, body forces, viscosity, shocks, and shaft work, total pressure and total temperature are constant along streamlines. This is because entropy is constant along a streamline, and, under the preceding assumptions, the first law of thermodynamics requires that the total enthalpy must be constant along a streamline. If both the entropy and total enthalpy are constant along a streamline, the stagnation state of the fluid cannot change along a streamline.

Secondly, it will be necessary to have an equation that permits the rotation to be evaluated from measurable properties. According to Crocco's theorem,[3]

$$\omega = \frac{1}{V}\left(\frac{\partial h_0}{\partial n} - T\frac{\partial s}{\partial n}\right) \tag{A1}$$

where the rotation $\omega$ is defined by

$$\omega \equiv \frac{\partial u}{\partial r} - \frac{\partial v}{\partial x}$$

A basic thermodynamic relationship involving entropy is

$$Tds = dh - (1/\rho)dP$$

from which it follows that

$$T_0\frac{\partial s_0}{\partial n} = \frac{\partial h_0}{\partial n} - \frac{1}{\rho_0}\frac{\partial P_0}{\partial n} \tag{A2}$$

By the definition of the stagnation state, $s_0 = s$. Thus, combining (A1) and (A2) gives

$$\omega = \frac{1}{V}\left[\frac{\partial h_0}{\partial n} - \frac{T}{T_0}\left(\frac{\partial h_0}{\partial n} - \frac{1}{\rho_0}\frac{\partial P_0}{\partial n}\right)\right] \tag{A3}$$

From conservation of energy,

$$T/T_0 = 1 - [(\gamma - 1)/2]M_0^2$$

Introducing this into Eq. (A3) gives

$$\omega = \frac{1}{V}\left[\frac{\partial h_0}{\partial n} - \left(1 - \frac{\gamma - 1}{2}M_0^2\right)\left(\frac{\partial h_0}{\partial n} - \frac{1}{\rho_0}\frac{\partial P_0}{\partial n}\right)\right]$$

Using the following perfect gas (ideal gas, constant specific heats) relationships

$$V = M_0\sqrt{\gamma R T_0} \qquad \frac{\partial h_0}{\partial n} = C_P\frac{\partial T_0}{\partial n} \qquad C_P = \frac{\gamma R}{\gamma - 1}$$

yields

$$\omega = \frac{1}{M_0\sqrt{\gamma R T_0}}\left[\frac{\gamma R M_0^2}{2}\frac{\partial T_0}{\partial n} + \left(1 - \frac{\gamma - 1}{2}M_0^2\right)\frac{1}{\rho_0}\frac{\partial P_0}{\partial n}\right] \tag{A4}$$

Since measurements of stagnation conditions normally are conducted in the $x$-$r$ coordinate system, it is necessary to convert this equation from the streamline coordinate system to the $x$-$r$ coordinate system. This is done by application of

the chain rule and the previously discussed fact that total pressure and total temperature are constant along streamlines. Therefore,

$$\frac{\partial T_0}{\partial s} = \frac{\partial T_0}{\partial x}\frac{\partial x}{\partial s} + \frac{\partial T_0}{\partial r}\frac{\partial r}{\partial s} = 0 \tag{A5}$$

$$\frac{\partial T_0}{\partial n} = \frac{\partial T_0}{\partial x}\frac{\partial x}{\partial n} + \frac{\partial T_0}{\partial r}\frac{\partial r}{\partial n} \tag{A6}$$

Applying the coordinate transformation equations

$$\frac{\partial r}{\partial s} = \frac{v}{V} \qquad \frac{\partial x}{\partial s} = \frac{u}{V}$$

$$\frac{\partial r}{\partial n} = \frac{u}{V} \qquad \frac{\partial x}{\partial n} = -\frac{u}{V}$$

to Eqs. (A5) and (A6) yields

$$\frac{\partial T_0}{\partial x} = -\frac{v}{u}\frac{\partial T_0}{\partial r} \qquad \frac{\partial T_0}{\partial n} = \frac{V}{u}\frac{\partial T_0}{\partial r} \tag{A7}$$

Likewise, for total pressure,

$$\frac{\partial P_0}{\partial n} = \frac{V}{u}\frac{\partial P_0}{\partial r}$$

Thus Eq. (A4) becomes

$$\omega = \frac{V/u}{M_0\sqrt{\gamma R T_0}}\left[\frac{\gamma R M_0^2}{2}\frac{\partial T_0}{\partial r} + \left(1 - \frac{\gamma - 1}{2}M_0{}^2\right)\frac{1}{\rho_0}\frac{\partial P_0}{\partial r}\right]$$

It is convenient to nondimensionalize all variables in this equation with respect to the stagnation speed of sound $c_0$ and the radius of the outer wall at the throat $R_{\text{th}}$. Accordingly, the following relationships are employed:

$$\hat{u} \equiv \frac{u}{c_0} = \frac{u}{\sqrt{\gamma R T_0}} \qquad \hat{v} \equiv \frac{v}{c_0} = \frac{v}{\sqrt{\gamma R T_0}}$$

$$\hat{x} \equiv \frac{x}{R_{\text{th}}} \qquad \hat{r} \equiv \frac{r}{R_{\text{th}}}$$

From the definition of rotation,

$$\omega \equiv \frac{\partial u}{\partial r} - \frac{\partial v}{\partial x} = \frac{1}{R_{\text{th}}}\left[\frac{\partial(\hat{u}\sqrt{\gamma R T_0})}{\partial \hat{r}} - \frac{\partial(\hat{v}\sqrt{\gamma R T_0})}{\partial \hat{x}}\right] \tag{A8}$$

Expanding and using Eq. (A7) yields

$$\omega = \frac{1}{2R_{\text{th}}}\sqrt{\frac{\gamma R}{T_0}}\left[2T_0\left(\frac{\partial \hat{u}}{\partial \hat{r}} - \frac{\partial \hat{v}}{\partial \hat{x}}\right) + \frac{M_0{}^2}{\hat{u}}\frac{\partial T_0}{\partial \hat{r}}\right] \tag{A9}$$

Equating the right-hand sides of Eqs. (A8) and (A9) yields, after simplification,

$$2T_0\left(\frac{\partial \hat{u}}{\partial \hat{r}} - \frac{\partial \hat{v}}{\partial \hat{x}}\right) + \frac{M_0{}^2}{\hat{u}}\frac{\partial T_0}{\partial \hat{r}} = \frac{1}{\hat{u}}\left[M_0{}^2\frac{\partial T_0}{\partial \hat{r}} + \frac{2}{\gamma}\left(1 - \frac{\gamma - 1}{2}M_0{}^2\right)\frac{T_0}{P_0}\frac{\partial P_0}{\partial \hat{r}}\right]$$

or

$$\frac{\partial \hat{u}}{\partial \hat{r}} - \frac{\partial \hat{v}}{\partial \hat{x}} = \left(1 - \frac{\gamma - 1}{2}M_0{}^2\right)\frac{1}{\hat{u}\gamma P_0}\frac{\partial P_0}{\partial r}$$

Now, since

$$\hat{\omega} \equiv \frac{\partial \hat{u}}{\partial \hat{r}} - \frac{\partial \hat{v}}{\partial \hat{r}}$$

then

$$\hat{\omega} = \left(1 - \frac{\gamma - 1}{2}M_0{}^2\right)\frac{1}{\hat{u}\gamma P_0}\frac{\partial P_0}{\partial \hat{r}} \tag{A10}$$

Having completed these preliminaries, it is possible to derive the equation satisfied by the velocity function. In cylindrical coordinates, the continuity equation for steady flow is

$$\frac{1}{r}\frac{\partial}{\partial r}(r\rho v) + \frac{1}{r}\frac{\partial}{\partial \theta}(\rho w) + \frac{\partial}{\partial x}(\rho u) = 0$$

For axisymmetric flow,

$$w = 0 \qquad \frac{\partial}{\partial \theta} = 0$$

which permits the simplified continuity equation

$$\frac{1}{r}\frac{\partial}{\partial r}(r\rho v) + \frac{\partial}{\partial x}(\rho u) = 0$$

to be written. Expanding gives

$$u\frac{\partial \rho}{\partial x} + v\frac{\partial \rho}{\partial r} + \rho\left(\frac{\partial u}{\partial x} + \frac{\partial v}{\partial r} + \frac{v}{r}\right) = 0 \tag{A11}$$

Examining the first two terms of this equation, it can be noted that

$$u\frac{\partial \rho}{\partial x} + v\frac{\partial \rho}{\partial r} = \frac{\mathrm{D}\rho}{\mathrm{D}t}$$

for steady flow. Since density can be expressed as a function of pressure and entropy, the chain rule yields

$$\frac{\mathrm{D}\rho}{\mathrm{D}t} = \frac{\partial \rho}{\partial P}\bigg|_s \frac{\mathrm{D}P}{\mathrm{D}t} + \frac{\partial \rho}{\partial s}\bigg|_P \frac{\mathrm{D}s}{\mathrm{D}t} \tag{A12}$$

However, because entropy is constant along a streamline, $\mathrm{D}s/\mathrm{D}t$ is zero. Noting that the sonic speed is defined by the equation

$$c^2 \equiv \frac{\partial P}{\partial \rho}\bigg|_s$$

Eq. (A12) can be reduced to

$$\frac{\mathrm{D}\rho}{\mathrm{D}t} = \frac{1}{c^2}\frac{\mathrm{D}P}{\mathrm{D}t} \tag{A13}$$

Euler's equation for isentropic flow along a streamline,

$$\mathrm{d}P = -\rho\frac{\mathrm{d}V^2}{2}$$

yields

$$\frac{\mathrm{D}P}{\mathrm{D}t} = \frac{\rho}{2}\frac{\mathrm{D}V^2}{\mathrm{D}t}$$

Therefore, Eq. (A13) becomes

$$\frac{D\rho}{Dt} = -\frac{\rho}{2c^2}\frac{DV^2}{Dt}$$

Expressing this equation in terms of the velocity components results in

$$\frac{D\rho}{Dt} = -\frac{\rho}{c^2}\left[u^2\frac{\partial u}{\partial x} + v^2\frac{\partial v}{\partial r} + uv\left(\frac{\partial u}{\partial r} + \frac{\partial v}{\partial x}\right)\right]$$

Substituting this into Eq. (A11) and rearranging gives

$$(c^2-u^2)\frac{\partial u}{\partial x} + (c^2-v^2)\frac{\partial v}{\partial r} - uv\left(\frac{\partial u}{\partial r} + \frac{\partial v}{\partial x}\right) + \frac{c^2 v}{r} = 0$$

Using the same procedure as in the previous section, this equation can be nondimensionalized. This gives

$$(\hat{c}^2-\hat{u}^2)\frac{\partial \hat{u}}{\partial \hat{x}} + (\hat{c}^2-\hat{v}^2)\frac{\partial \hat{v}}{\partial \hat{r}} - \hat{u}\hat{v}\left(\frac{\partial \hat{u}}{\partial \hat{x}} + \frac{\partial \hat{v}}{\partial \hat{x}}\right) + \frac{\hat{c}^2\hat{v}}{\hat{r}}$$

$$+ \frac{R_{th}}{c_0{}^2}(\hat{c}^2 - M_0{}^2)\left(u\frac{\partial c_0}{\partial x} + v\frac{\partial c_0}{\partial r}\right) = 0 \qquad \text{(A14)}$$

where

$$\hat{c}^2 \equiv c^2/c_0{}^2 = 1 - [(\gamma-1)/2]M_0{}^2$$

Examining the last term of Eq. (A14) reveals

$$u\frac{\partial c_0}{\partial x} + v\frac{\partial c_0}{\partial r} = \frac{Dc_0}{Dt}$$

for steady flow. The substantial derivative is the rate of change of a property for a fluid particle as it moves along a streamline. However, it was shown that all stagnation properties are constant along streamlines. Therefore,

$$\frac{Dc_0}{DT} = 0$$

Equation (A14) reduces to

$$(\hat{c}^2-\hat{u}^2)\frac{\partial \hat{u}}{\partial \hat{x}} + (\hat{c}^2-\hat{v}^2)\frac{\partial \hat{v}}{\partial \hat{r}}$$

$$- \hat{u}\hat{v}\left(\frac{\partial \hat{u}}{\partial \hat{r}} + \frac{\partial \hat{v}}{\partial \hat{x}}\right) + \frac{\hat{c}^2\hat{v}}{\hat{r}} = 0 \qquad \text{(A15)}$$

Let $\phi$ and $F$ be functions such that

$$\phi_{\hat{x}} + F \equiv \hat{u} \qquad \text{(A16)}$$

$$\phi_{\hat{r}} \equiv \hat{v} \qquad \text{(A17)}$$

By differentiating Eq. (A16) by $r$ and Eq. (A17) by $x$ and subtracting the results, it can be shown that $F_{\hat{r}} = \omega$. Substituting Eqs. (A16) and (A17) into Eq. (A15) yields the velocity function equation:

$$[\hat{c}^2 - (\phi_{\hat{x}} + F)](\phi_{\hat{x}\hat{x}} + F_{\hat{x}}) + [\hat{c}^2 - (\phi_{\hat{r}})^2](\phi_{\hat{r}\hat{r}})$$

$$- (\phi_{\hat{x}} + F)(\phi_{\hat{r}})(2\phi_{\hat{x}\hat{r}} + F_{\hat{r}}) + \hat{c}^2(\phi_{\hat{r}}/\hat{r}) = 0$$

## Acknowledgment

This work was sponsored by the Douglas Aircraft Co., McDonnell Douglas Corp., and was performed under their Independent Research and Development Program. The Douglas principle investigator was G. L. Hamilton.

## References

[1] Wehofer, S. and Matz, R. J., "Turbine Engine Exhaust Nozzle Performance," AIAA Paper 73-1302, 1973.

[2] Brown, E. F. and Hamilton, G. L., "A Survey of Methods for Exhaust-Nozzle Flow Analysis," *Journal of Aircraft*, Vol. 13, Jan. 1976, pp. 4-11.

[3] Shapiro, A. H., *The Dynamics and Thermodynamics of Compressible Fluid Flow*, Ronald Press Co., New York, 1953, p. 282.

[4] Ferri, A. and Dash, S., "The Calculation of Nozzle Discharge Coefficients Accounting for Viscosity Losses and Flow Nonuniformities," Advanced Technology Labs., Jericho, N. Y., Rept. ATL TR 160, Oct. 1970.

[5] Wehofer, S. and Moger, W. C., "Analysis and Computer Program for Evaluation of Air-Breathing Propulsion Exhaust Nozzle Performance," ARO, Inc., Arnold Air Force Station, Tenn., AEDC-TR-73-29, 1973.

[6] Wehofer, S. and Moger, W. C., "Transonic Flow in Conical Convergent and Convergent-Divergent Nozzles with Nonuniform Entrance Conditions," AIAA Paper 70-635, 1970.

[7] Emmons, H. W., "The Numerical Solution of Compressible Fluid Flow Problems," NACA TN, 932, 1944.

[8] Murman, E. M. and Cole, J. D., "Calculation of Plane Steady Transonic Flows," AIAA Paper 70-188, 1970.

[9] Taulbee, D. B. and Boraas, S., "Transonic Nozzle Flow with Nonuniform Total Energy," *AIAA Journal*, Vol. 9, Oct. 1971, pp. 2102-2104.

[10] Roache, P. J., *Computational Fluid Dynamics*, Hermosa Publishers, Albuquerque, N. Mex., 1972, pp. 290-301.

[11] South, J. C. Jr. and Jameson, A., "Relaxation Solutions for Inviscid Axisymmetric Transonic Flow Over Blunt or Pointed Bodies," *Proceedings AIAA Computational Fluid Dynamics Conference*, 1973, pp. 8-17.

[12] Oswatitsch, K. and Rothstein, W., "Flow Patterns in a Converging-Diverging Nozzle," NACA Tech. Memo. 1215, 1949.